Hindawi Publishing Corporation
Journal of Mathematics
Volume 2013, Article ID 583615, 10 pages
http://dx.doi.org/10.1155/2013/583615

Research Article

Effect of Internal Heat Generation/Absorption on Dusty Fluid Flow over an Exponentially Stretching Sheet with Viscous Dissipation

G. M. Pavithra and B. J. Gireesha

Department of Studies and Research in Mathematics, Kuvempu University, Shankaraghatta, Shimoga, Karnataka 577 451, India

Correspondence should be addressed to B. J. Gireesha; bjgireesu@rediffmail.com

Received 8 January 2013; Accepted 2 June 2013

Academic Editor: Pierpaolo D'Urso

A numerical analysis has been carried out to describe the boundary layer flow and heat transfer of a dusty fluid over an exponentially stretching surface in the presence of viscous dissipation and internal heat generation/absorption. The governing partial differential equations are reduced to nonlinear ordinary differential equations by a similarity transformation, before being solved numerically by Runge-Kutta-Fehlberg 45 method. The heat transfer analysis has been carried out for both PEST and PEHF cases. The numerical results are compared with the earlier study and found to be in excellent agreement. Some important features of the flow and heat transfer in terms of velocities and temperature distributions for different values of the governing parameters like fluid-particle interaction parameter, Prandtl number, Eckert number, Number density, heat source/sink parameter, and suction parameter which are of physical and engineering interests are analyzed, discussed, and presented through tables and graphs.

1. Introduction

An investigation on boundary layer flow and heat transfer of viscous fluids over a moving continuous stretching surface has considerable practical applications in industries and engineering, since the study of heat transfer has become important industrially for determining the quality of final product which greatly depends on the rate of cooling. Many researchers inspired by Sakiadis [1, 2] who initiated the boundary layer behavior studied the stretching flow problem in various aspects. Extension to that, an exact solution was given by Crane [3] for a boundary layer flow caused by stretching surface. A new dimension to the boundary layer flow was given by Magyari and Keller [4] by considering the nonstandard stretching flow known as exponentially stretching surface. They described the mass and heat transfer characteristics of the boundary layer. After that, Elbashbeshy [5] was the first who considered the heat transfer problem over an exponentially stretching sheet with suction parameter. The effect of viscous dissipation on the boundary layer flow along vertical exponential stretching sheet was explained by Partha et al. [6].

Sanjayanand and Khan [7] discussed heat and mass transfer in a viscoelastic boundary layer flow over an exponentially stretching sheet. The numerical solution for the boundary layer flow with thermal radiation over an exponentially stretching sheet was given by Bidin and Nazar [8]. Samad and Mohebujjaman [9] worked on both heat and mass transfer of free convective flow along a vertical stretching sheet in presence of magnetic field with heat generation. Again Elbashbeshy and Aldawody [10] investigated the heat transfer over an unsteady stretching surface embedded in a porous medium with variable heat flux in the presence of heat source or sink. Ishak [11] and Bala and Bhaskar [12] discussed the boundary layer flow over an exponentially stretching sheet with magnetic field and thermal radiation effect. On the other hand, Sahoo and Poncet [13] carried out an exponentially stretching flow problem by considering partial slip boundary condition for third grade fluid. The flow and heat transfer of a Jeffrey fluid past an exponentially stretching sheet with thermal radiation is analyzed by Nadeem et al. [14]. Kumar [15] discussed the heat transfer over a stretching porous sheet subjected to power law heat flux in presence of heat source.

Very recently Bhattacharyya [16] analyzed the effects of radiation and heat source/sink on unsteady MHD boundary layer flow and heat transfer over a shrinking sheet with suction/injection.

All the works as mentioned above are restricted only for fluids induced by stretching sheet. In fact, a fluid flow with dust particles is a significant type of flow due to its wide range of its applications in the boundary layer that include the use of dust in gas cooling systems, centrifugal separation of matter from fluid, polymer technology, and fluid droplets sprays, that is, powder technology and paint spraying. The fluid-particle system was initially described by Saffman [17] and derived the motion of gas equations carrying the dust particles. Further, Datta and Mishra [18] have investigated dusty fluid in boundary layer flow over a semi-infinite flat plate. Gireesha et al. [19] have obtained the boundary layer and heat transfer of a dusty fluid flow over a stretching sheet with nonuniform heat source/sink and concluded that the temperature dependent heat sinks are better suited for cooling purposes. Also Gireesha et al. [20, 21] have discussed the boundary layer flow and heat transfer of a dusty fluid over a stretching sheet by considering the viscous dissipation for both steady and unsteady flows.

On basis of previous observations, we have considered the flow over an exponentially stretching sheet. The main aim of the present investigation is to study the effect of viscous dissipation and internal heat generation/absorption on flow and heat transfer of a dusty fluid over an exponentially stretching sheet with suction parameter by taking PEST and PEHF cases. The study of heat generation or absorption in moving fluids is important in problems dealing with chemical reactions and these concerned with dissociating fluids. Flows in porous media have several applications in geothermal, oil reservoir engineering, and astrophysics. The governing boundary layer equations have been simplified using suitable similarity transformations and then have been solved numerically using Runge-Kutta-Fehlberg 45 method with the help of Maple.

2. Mathematical Formulation and Solution of the Problem

A steady two-dimensional laminar boundary layer flow and heat transfer of an incompressible viscous dusty fluid near a permeable plane wall stretching with velocity $U_w = U_0 e^{(x/L)}$ is considered (Figure 1). The x-axis is chosen along the sheet and y-axis normal to it. Two equal and opposite forces are applied along the sheet, so that the wall is stretched exponentially.

Under these assumptions, the two-dimensional boundary layer equations can be written as

$$\frac{\partial u}{\partial x} + \frac{\partial v}{\partial y} = 0, \tag{1}$$

$$u\frac{\partial u}{\partial x} + v\frac{\partial u}{\partial y} = \upsilon\frac{\partial^2 u}{\partial y^2} + \frac{KN}{\rho}\left(u_p - u\right), \tag{2}$$

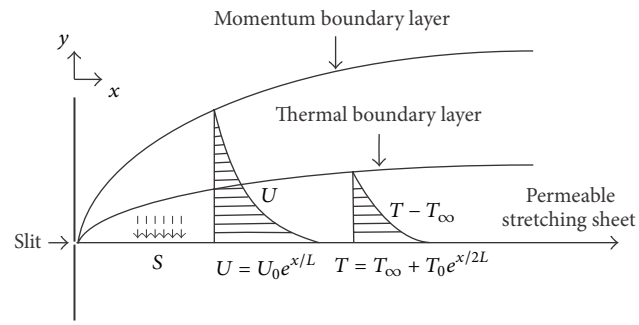

Figure 1: Schematic representation of boundary layer flow.

$$\frac{\partial u_p}{\partial x} + \frac{\partial v_p}{\partial y} = 0, \tag{3}$$

$$u_p\frac{\partial u_p}{\partial x} + v_p\frac{\partial u_p}{\partial y} = \frac{K}{m}\left(u - u_p\right), \tag{4}$$

where x and y represent coordinate axes along the continuous surface in the direction of motion and perpendicular to it, respectively. (u, v) and (u_p, v_p) denote the velocity components of the fluid and particle phase along the x and y directions, respectively, υ is the coefficient of viscosity of fluid, ρ is the density of the fluid phase, K is Stoke's resistance, N is the number density of dust particles, m is the mass concentration of dust particles, and $\tau_v = m/K$ is the relaxation time of particle phase.

In order to solve the governing boundary layer equations, consider the following appropriate boundary conditions on velocity:

$$\begin{gathered} u = U_w(x), \quad v = V_w(x) \quad \text{at } y = 0, \\ u \longrightarrow 0, \quad u_p \longrightarrow 0, \quad v_p \longrightarrow v, \quad \text{as } y \longrightarrow \infty, \end{gathered} \tag{5}$$

where $U_w(x) = U_0 e^{(x/L)}$ is the sheet velocity, $V_w(x) = -S\sqrt{U_0\upsilon/2L}e^{(x/2L)}$ is the suction velocity, U_0 is reference velocity, and L is the reference length.

Equations (1)–(4) that are subject to boundary condition (5) admit self-similar solutions in terms of the similarity function f and the similarity variable η as

$$\begin{gathered} u = U_0 e^{x/L} f'(\eta), \\ v = -\sqrt{\frac{u_0\upsilon}{2L}}e^{x/2L}\left[f(\eta) + \eta f'(\eta)\right], \\ u_p = U_0 e^{x/L} F'(\eta), \\ v_p = -\sqrt{\frac{u_0\upsilon}{2L}}e^{x/2L}\left[F(\eta) + \eta F'(\eta)\right], \\ \eta = \sqrt{\frac{u_0}{2\upsilon L}}e^{x/2L} y. \end{gathered} \tag{6}$$

Table 1: Comparison of the results for the dimensionless wall temperature gradient $\theta'(0)$ (PEST case) by varying the Pr and Ec with $\beta = N = \lambda = S = 0$.

Pr	Ec = 0			Ec = 0.2			Ec = 0.9		
	Nadeem et al. [14]	Bidin and Nazar [8]	Present study $\theta'(0)$	Nadeem et al. [14]	Bidin and Nazar [8]	Present study $\theta'(0)$	Nadeem et al. [14]	Bidin and Nazar [8]	Present study $\theta'(0)$
1	−0.955	−0.955	−0.955	−0.863	−0.862	−0.863	−0.539	−0.539	−0.539
2	−1.471	−1.471	−1.471	−1.306	−1.306	−1.305	−0.725	−0.725	−0.724
3	−1.870	−1.869	−1.869	−1.639	−1.688	−1.638	−0.830	−0.830	−0.830

Table 2: Values of wall temperature gradient $\theta'(0)$ (for PEST case) and wall temperature $\theta(0)$ (for PEHF case).

β	Pr	Ec	λ	N	$\theta'(0)$	$\theta(0)$
0.2					−1.75024	0.63348
0.6	0.72	0.5	0.5	0.5	−1.66464	0.67408
1.0					−1.64077	0.68511
	0.72				−1.66464	0.67408
0.6	1.0	0.5	0.5	0.5	−2.01014	0.59634
	1.5				−2.53037	0.52418
		0			−2.03930	0.49036
0.6	0.72	0.5	0.5	0.5	−1.66464	0.67408
		1.0			−1.28998	0.85780
			0.5		−1.66464	0.67408
0.6	0.72	0.5	1.0	0.5	−1.39884	0.77824
			1.5		−1.05000	0.96894
				0.5	−1.66464	0.67408
0.6	0.72	0.5	0.5	1.0	−2.39962	0.51431
				1.5	−2.94768	0.44797

These equations identically satisfy the governing equations (1) and (3). Substitute (6) into (2)–(4) and on equating the coefficient of $(x \setminus L)^0$ on both sides, and then one can get

$$f'''(\eta) + f(\eta) f''(\eta) - 2f'(\eta)^2 + 2l\beta\left[F'(\eta) - f'(\eta)\right] = 0,$$
$$F(\eta) F''(\eta) - 2F'(\eta)^2 + 2\beta\left[f'(\eta) - F'(\eta)\right] = 0, \tag{7}$$

where prime denotes the differentiation with respect to η, $l = mN/\rho$ is the mass concentration, and $\beta = L/\tau_v U_0$ is the fluid-particle interaction parameter for velocity.

Similarity boundary conditions (5) will become

$$f'(\eta) = 1, \quad f(\eta) = S \quad \text{at } \eta = 0,$$
$$f'(\eta) = 0, \qquad F'(\eta) = 0, \tag{8}$$
$$F(\eta) = f(\eta) + \eta f'(\eta) - \eta F'(\eta) \quad \text{as } \eta \longrightarrow \infty,$$

where $S > 0$ is a suction parameter.

The important physical parameter for the boundary layer flow is the skin-friction coefficient which is defined as

$$C_f = \frac{\tau_w}{\rho U_w^2}, \tag{9}$$

where the skin friction τ_w is given by

$$\tau_w = \mu\left(\frac{\partial u}{\partial y}\right)_{y=0}. \tag{10}$$

Table 3: Values of skin friction coefficient $f''(0)$.

β	S	$f''(0)$
0.2		−1.55365
0.6	0.5	−1.56928
1.0		−1.57897
	0.5	−1.56928
0.6	1.0	−1.88171
	1.5	−2.23651

Using the nondimensional variables, one obtains

$$\sqrt{2\,\mathrm{Re}\,C_f} = f''(0), \tag{11}$$

where $\mathrm{Re} = U_0 L/v$ is the Reynolds number.

3. Heat Transfer Analysis

The governing steady, boundary layer heat transport equations for both fluid and dust phases with viscous dissipation and heat generation/absorption are given by

$$\rho c_p\left[u\frac{\partial T}{\partial x} + v\frac{\partial T}{\partial y}\right] = k\frac{\partial^2 T}{\partial y^2} + \frac{Nc_p}{\tau_T}\left(T_p - T\right) + \frac{N}{\tau_v}\left(u_p - u\right)^2 + \mu\left(\frac{\partial u}{\partial y}\right)^2 + Q\left(T - T_\infty\right),$$
$$Nc_m\left[u_p\frac{\partial T_p}{\partial x} + v_p\frac{\partial T_p}{\partial y}\right] = -\frac{Nc_p}{\tau_T}\left(T_p - T\right), \tag{12}$$

where T and T_p are the temperatures of the fluid and dust particles inside the boundary layer, c_p and c_m are the specific heat of fluid and dust particles, τ_T is the thermal equilibrium time; that is, it is time required by a dust cloud to adjust its temperature to the fluid, k is the thermal conductivity, τ_v is the relaxation time of the of dust particle, that is, the time required by a dust particle to adjust its velocity relative to the fluid, and Q represents the heat source when $Q > 0$ and the sink when $Q < 0$.

We solved the heat transfer phenomenon for two types of heating process, namely,

(1) prescribed exponential order surface temperature (PEST);

(2) prescribed exponential order heat flux (PEHF).

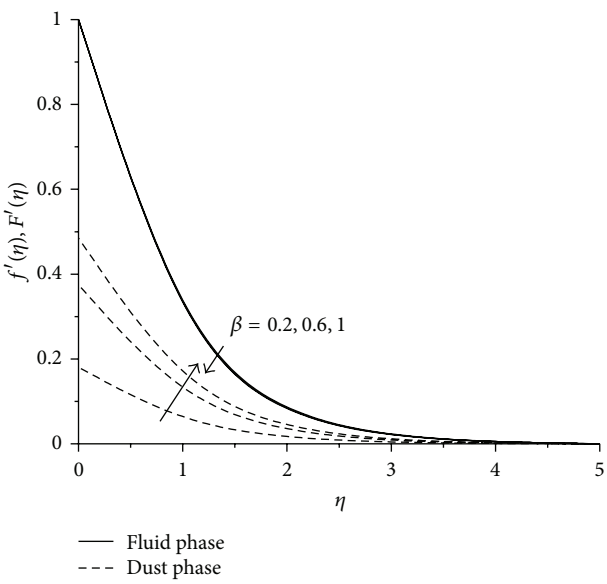

Figure 2: Effect of β on velocity profiles with $N = \lambda = \mathrm{Ec} = S = 0.5$ and $\mathrm{Pr} = 0.72$.

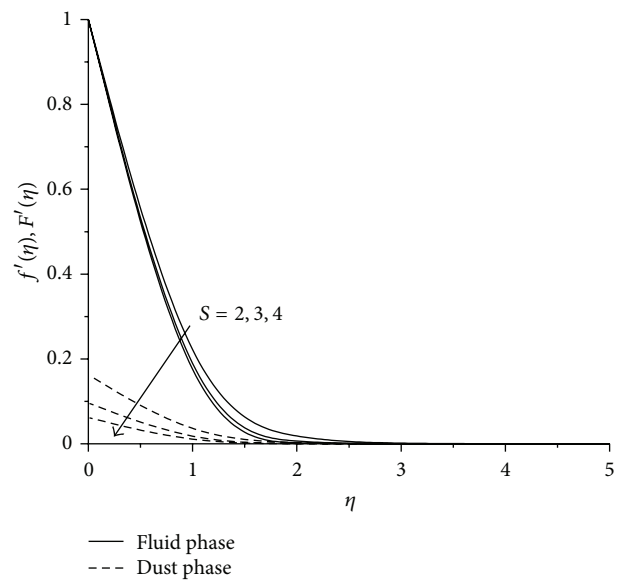

Figure 3: Effect of S on velocity profiles with $N = \lambda = \mathrm{Ec} = 0.5$, $\mathrm{Pr} = 0.72$, and $\beta = 0.6$.

Case 1 (prescribed exponential order surface temperature). For this heating process, we employ the following boundary conditions:

$$\begin{gathered} T = T_w(x) \quad \text{at } y = 0, \\ T \longrightarrow T_\infty, \quad T_p \longrightarrow T_\infty \quad \text{as } y \longrightarrow \infty, \end{gathered} \tag{13}$$

where $T_w = T_\infty + T_0 e^{c_1 x/2L}$ is the temperature distribution in the stretching surface, T_0 is a reference temperature, and c_1 is constant.

Introduce the dimensionless variables for the temperatures $\theta(\eta)$ and $\theta_p(\eta)$ as follows:

$$\theta(\eta) = \frac{T - T_\infty}{T_w - T_\infty}, \qquad \theta_p(\eta) = \frac{T_p - T_\infty}{T_w - T_\infty}, \tag{14}$$

where $T - T_\infty = T_0 e^{c_1 x/2L}\theta(\eta)$.

Using the similarity variable η and (14) into (12) and on equating the coefficient of $(x \setminus L)^0$ on both sides, one can arrive at the following system of equations:

$$\begin{aligned} &\theta''(\eta) + \mathrm{Pr}\left[f(\eta)\theta'(\eta) - c_1 f'(\eta)\theta(\eta)\right] \\ &\quad + \frac{2N}{\rho}\beta_T \mathrm{Pr}\left[\theta_p(\eta) - \theta(\eta)\right] \\ &\quad + \frac{2N}{\rho}\beta \mathrm{Pr}\,\mathrm{Ec}\left[F'(\eta) - f'(\eta)\right]^2 \\ &\quad + \mathrm{Pr}\,\mathrm{Ec}\left[f''(\eta)\right]^2 + 2\mathrm{Pr}\lambda\theta(\eta) = 0, \\ &c_1 F'(\eta)\theta_p(\eta) - F(\eta)\theta_p'(\eta) + 2\beta_T\gamma\left[\theta_p(\eta) - \theta(\eta)\right] = 0, \end{aligned} \tag{15}$$

where $\mathrm{Pr} = \mu c_p/k$ is the Prandtl number, $\mathrm{Ec} = U_0^2/c_p T$ is the Eckert number, $\beta = L/\tau_v U_0$ and $\beta_\tau = L/\tau_T U_0$ are the fluid-particle interaction parameter for velocity and temperature, and $\gamma = c_p/c_m$ is the ratio of specific heat.

Corresponding thermal boundary conditions becomes

$$\begin{gathered} \theta(\eta) = 1 \quad \text{at } \eta = 0, \\ \theta(\eta) \longrightarrow 0, \quad \theta_p(\eta) \longrightarrow 0 \quad \text{as } \eta \longrightarrow \infty. \end{gathered} \tag{16}$$

Case 2 (prescribed exponential order heat flux). For this heating process, consider the boundary conditions as follows:

$$\begin{gathered} \frac{\partial T}{\partial y} = -\frac{q_w(x)}{k} \quad \text{at } y = 0, \\ T \longrightarrow T_\infty, \qquad T_p \longrightarrow T_\infty \quad \text{as } \eta \longrightarrow \infty, \end{gathered} \tag{17}$$

where $q_w(x) = T_1 e^{(c_2+1)x/2L}$, T_1 is reference temperature, and c_2 is constant.

Using the similarity variable η and (14) into (12) and on equating the coefficient of $(x \setminus L)^0$ on both sides, one can arrive at the following system of equations:

$$\begin{aligned} &\theta''(\eta) + \mathrm{Pr}\left[f(\eta)\theta'(\eta) - c_1 f'(\eta)\theta(\eta)\right] \\ &\quad + \frac{2N}{\rho}\beta_T \mathrm{Pr}\left[\theta_p(\eta) - \theta(\eta)\right] \\ &\quad + \frac{2N}{\rho}\beta \mathrm{Pr}\,\mathrm{Ec}\left[F'(\eta) - f'(\eta)\right]^2 \\ &\quad + \mathrm{Pr}\,\mathrm{Ec}\left[f''(\eta)\right]^2 + 2\mathrm{Pr}\lambda\theta(\eta) = 0, \\ &c_1 F'(\eta)\theta_p(\eta) - F(\eta)\theta_p'(\eta) + 2\beta_T\gamma\left[\theta_p(\eta) - \theta(\eta)\right] = 0, \end{aligned} \tag{18}$$

where $\mathrm{Ec} = kU_0^2/c_p T_1\sqrt{U_0/2\upsilon L}$ is the Eckert number.

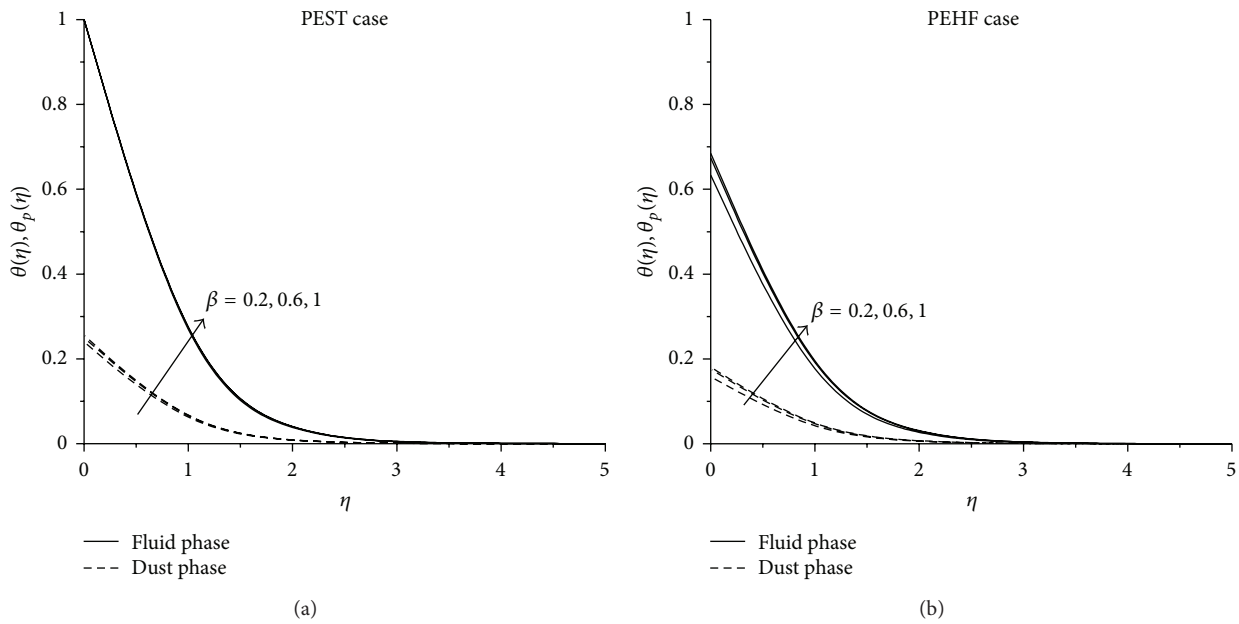

Figure 4: Effect of β on temperature profiles for both PEST and PEHF cases with $N = \lambda = \mathrm{Ec} = S = 0.5$ and $\mathrm{Pr} = 0.72$.

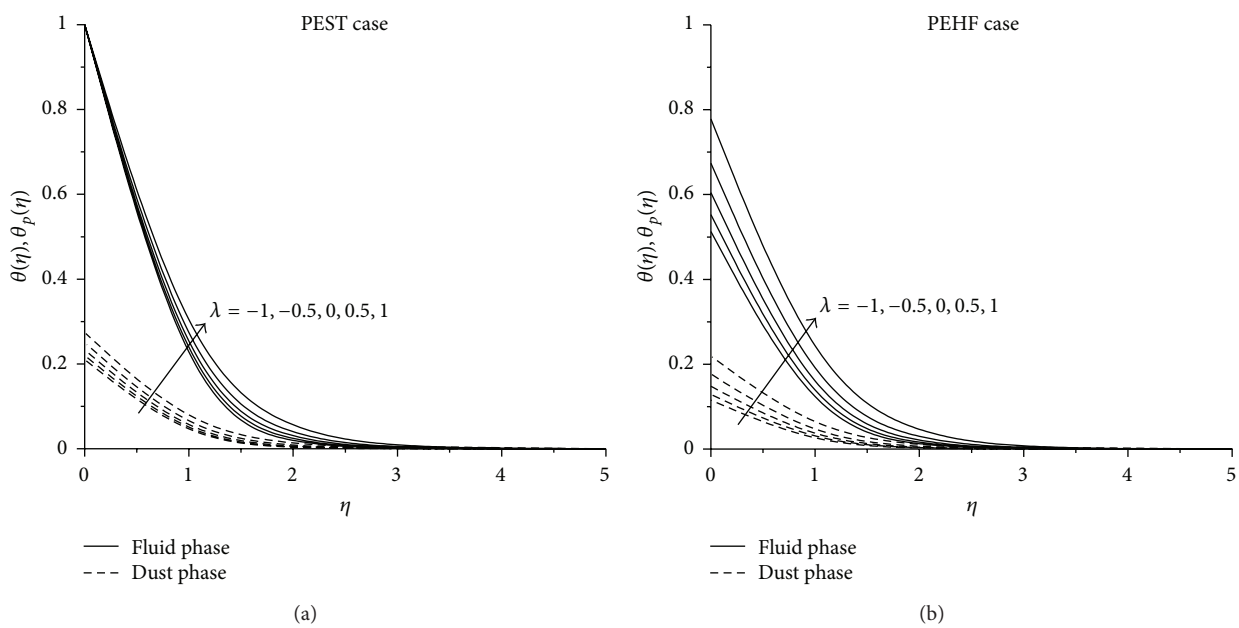

Figure 5: Effect of λ on temperature profiles for both PEST and PEHF cases with $N = \mathrm{Ec} = S = 0.5$, $\mathrm{Pr} = 0.72$, and $\beta = 0.6$.

Corresponding thermal boundary conditions becomes

$$\begin{gathered} \theta'(\eta) = -1 \quad \text{at } \eta = 0, \\ \theta(\eta) \longrightarrow 0, \quad \theta_p(\eta) \longrightarrow 0 \quad \text{as } \eta \longrightarrow \infty. \end{gathered} \tag{19}$$

4. Numerical Solution

Two-dimensional, boundary layer flow and heat transfer of a dusty fluid over an exponential stretching sheet is considered. The system of highly nonlinear ordinary differential equations (7), (15) for PEST case and (18) for PEHF case are solved numerically using RKF-45 method with the help of an algebraic software Maple. In this method, we choose suitable finite values of $\eta \to \infty$ as $\eta = 5$.

Here we have given the comparison of our results of $-\theta'(0)$ with Nadeem et al. [14] and Bidin and Nazar [8] as in Table 1 for various values of Pr and Ec. From this table, one can notice that there is a close agreement with these approaches and thus verifies the accuracy of the method used. The thermal characteristics at the wall that are examined for the values of temperature gradient $\theta'(0)$ in PEST case

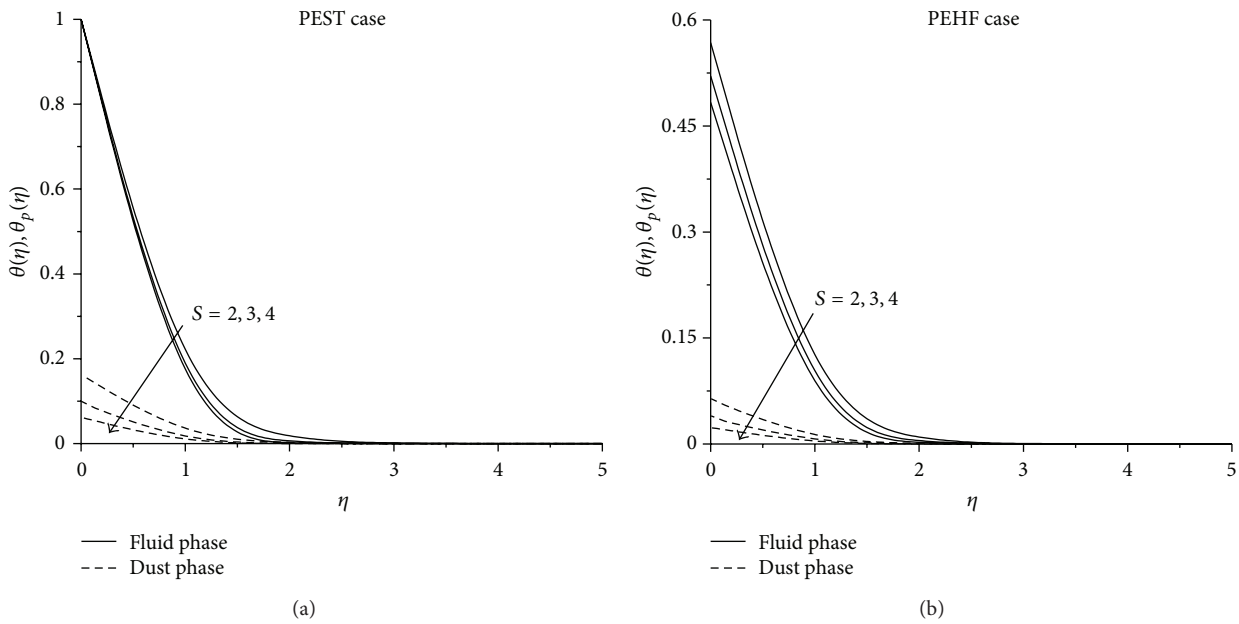

Figure 6: Effect of S on temperature profiles for both PEST and PEHF cases with $N = \text{Ec} = \lambda = 0.5$, $\text{Pr} = 0.72$, and $\beta = 0.6$.

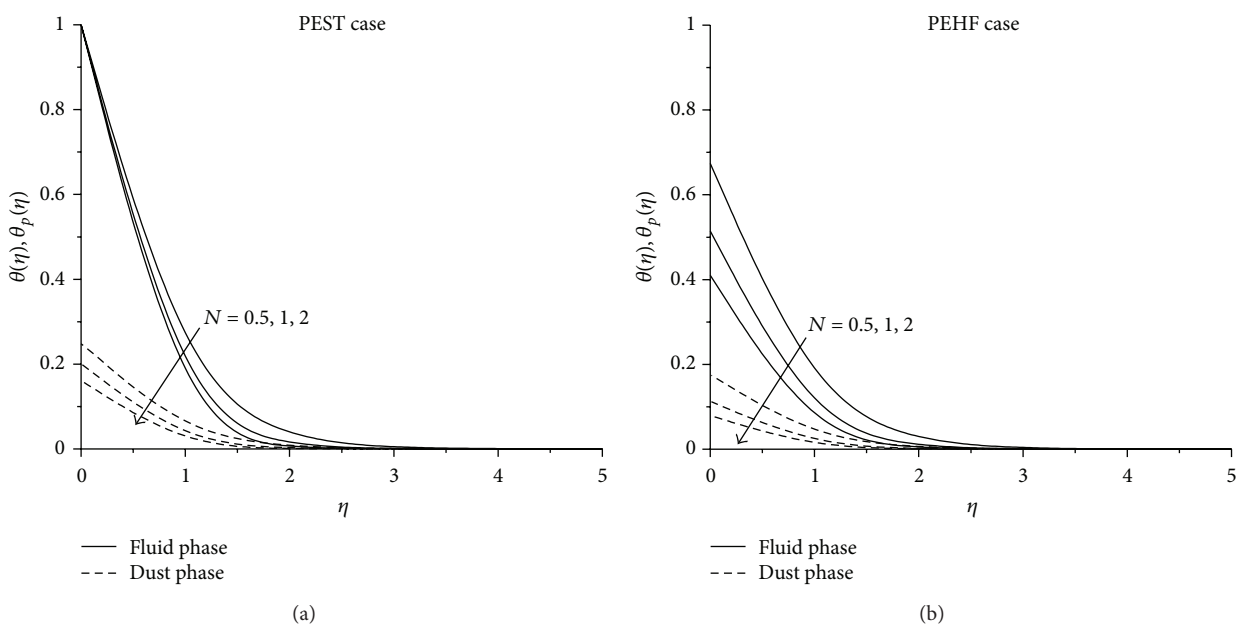

Figure 7: Effect of N on temperature profiles for both PEST and PEHF cases with $S = \text{Ec} = \lambda = 0.5$, $\text{Pr} = 0.72$, and $\beta = 0.6$.

and the temperature $\theta(0)$ in PEHF case are tabulated in Table 2. The computed values of skin friction coefficient $f''(0)$ is tabulated in Table 3 for different values of fluid-particle interaction parameter (β) and suction parameter (S). Further, we studied the effects of viscous dissipation and heat generation/absorption on velocity and temperature profiles that are depicted graphically for different values of fluid-particle interaction parameter (β), Suction parameter (S), heat source/sink parameter (λ), Number density (N), Prandtl number (Pr), and Eckert number (Ec).

5. Results and Discussion

Numerical calculations are performed for velocity and temperature profiles for various values of physical parameters such as fluid-particle interaction parameter (β), Suction parameter (S), heat source/sink parameter (λ), Number density (N), Prandtl number (Pr), and Eckert number (Ec) and are depicted graphically (from Figure 2 to Figure 11). Comparison values of wall-temperature gradient are tabulated in Table 1. From Table 3 we observed that the skin friction

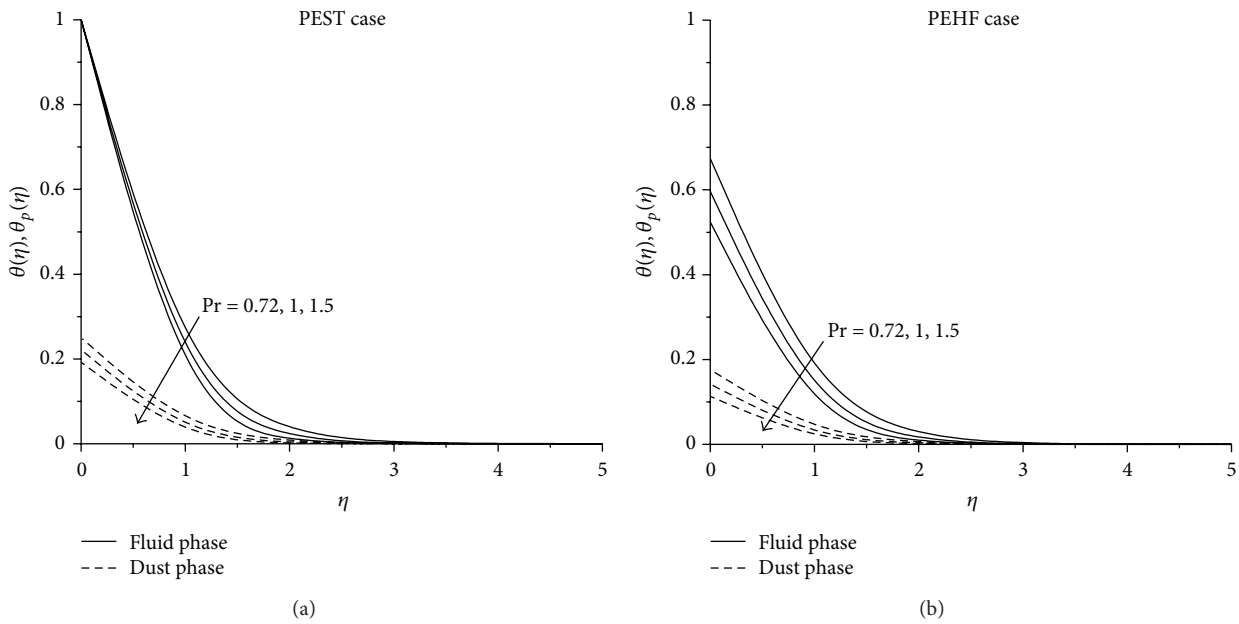

Figure 8: Effect of Pr on temperature profiles for both PEST and PEHF cases with $S = \mathrm{Ec} = N = \lambda = 0.5$ and $\beta = 0.6$.

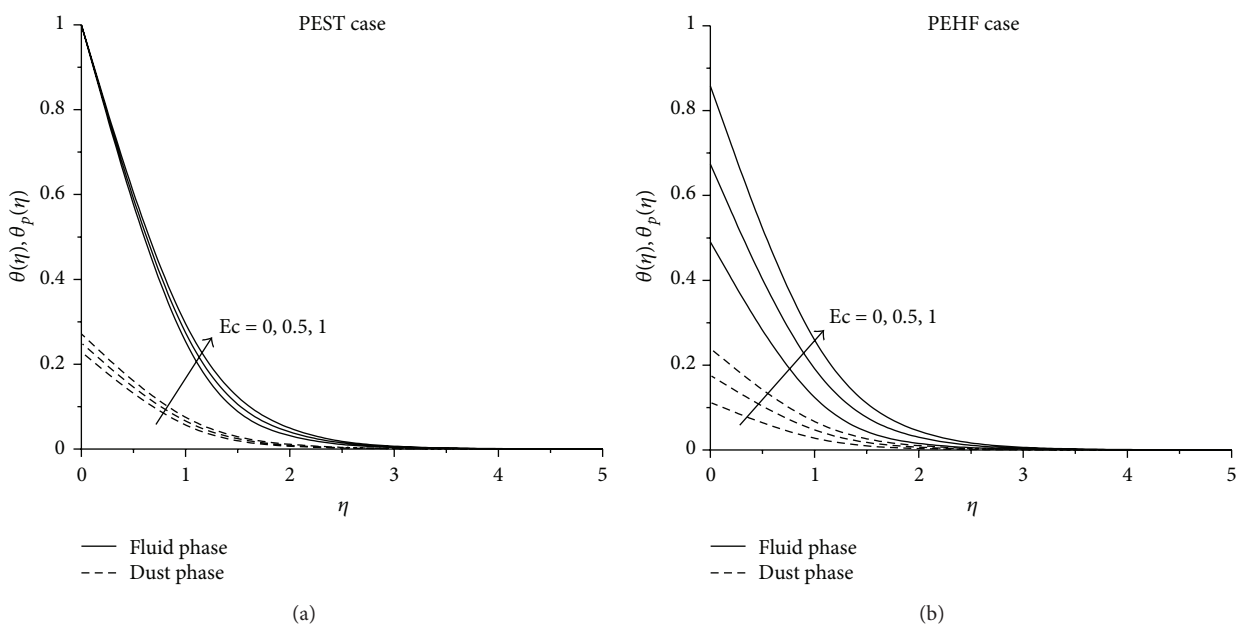

Figure 9: Effect of Ec on temperature profiles for both PEST and PEHF cases with $S = N = \lambda = 0.5$, $\mathrm{Pr} = 0.72$, and $\beta = 0.6$.

coefficient decreases with increasing values of fluid-particle interaction parameter (β) as well as for the suction parameter (S). Physically negative values of $f''(0)$ mean that the surface exerts a drag force on the fluid, so that the stretching surface will induce the flow.

From Figure 2, the observation shows that an increase in fluid-particle interaction parameter β decreases the fluid velocity $f'(\eta)$ and increases the particle velocity $F'(\eta)$, and also as β increases, the velocity of fluid will be equal to the velocity of the dust particle. Figure 3 represents the velocity profiles for different values of suction parameter S. It shows that the velocity of fluid and dust decreases when suction parameter increases. So that the momentum boundary layer thickness becomes thinner.

Figure 4 depicts the temperature profiles $\theta(\eta)$ and $\theta_p(\eta)$ versus η for different values of fluid-particle interaction parameter β. We infer from this figure that the temperature increase with increase in the fluid-particle interaction parameter β, and it indicates that the fluid-particle temperature is parallel to that of dust phase. Also one can observ that fluid phase temperature is higher than that of dust phase. From Figure 5, the observation shows the effect of heat source/sink

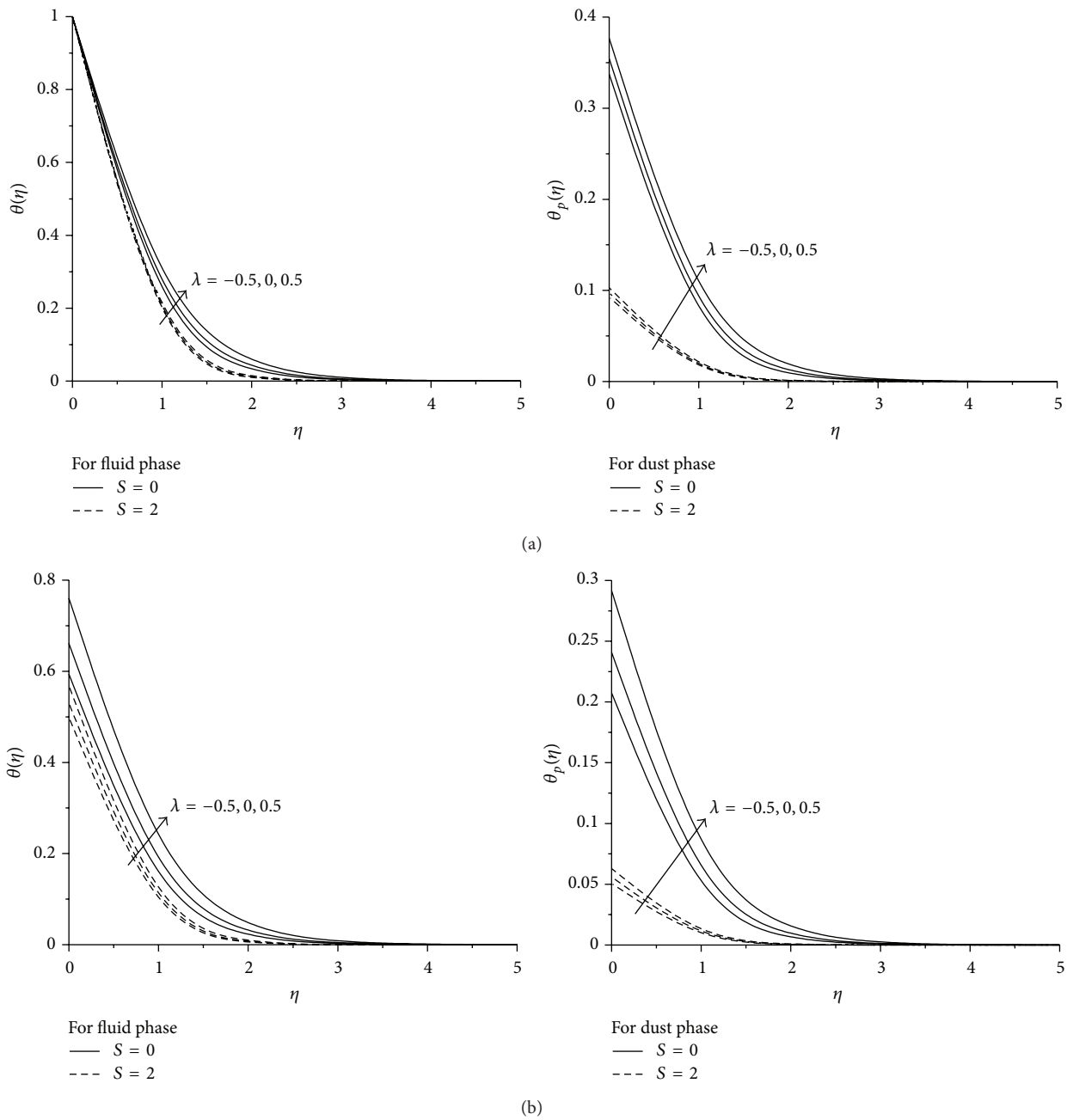

Figure 10: (a) Effect of λ on temperature profiles for PEST case; (b) effect of λ on temperature profiles for PEHF case.

parameter λ on temperature profiles. As λ increases, temperature profiles for both fluid and dust phases increase in both PEST and PEHF cases. It is clear that the temperature in the case of heat source is higher than in the case of sink. This is very much significant in which the heat transfer is given prime importance.

The effects of suction parameter S on the temperature profiles are depicted as in Figure 6. This figure explains that the temperature will decrease as S increases. This is due to the fact that the fluid at ambient conditions is brought closer to the surface which results in thinning of thermal boundary layer thickness. This causes an increase in the rate of heat transfer. So, suction can be used as a means for cooling the surface. Figure 7 shows the temperature distributions $\theta(\eta)$ and $\theta_p(\eta)$ versus η for different values of number density N. We infer from this figure that the temperature decreases with increases in N for both cases.

The temperature field for various values of the Prandtl number (Pr) is represent in Figure 8. The relative thickening of momentum and thermal boundary layers is controlled by Prandtl number (Pr). Since small values of Pr will possess higher thermal conductivities, so that heat can diffuse from the sheet very quickly compared to the velocity. From this figure, it reveals that the temperature decreases with increase

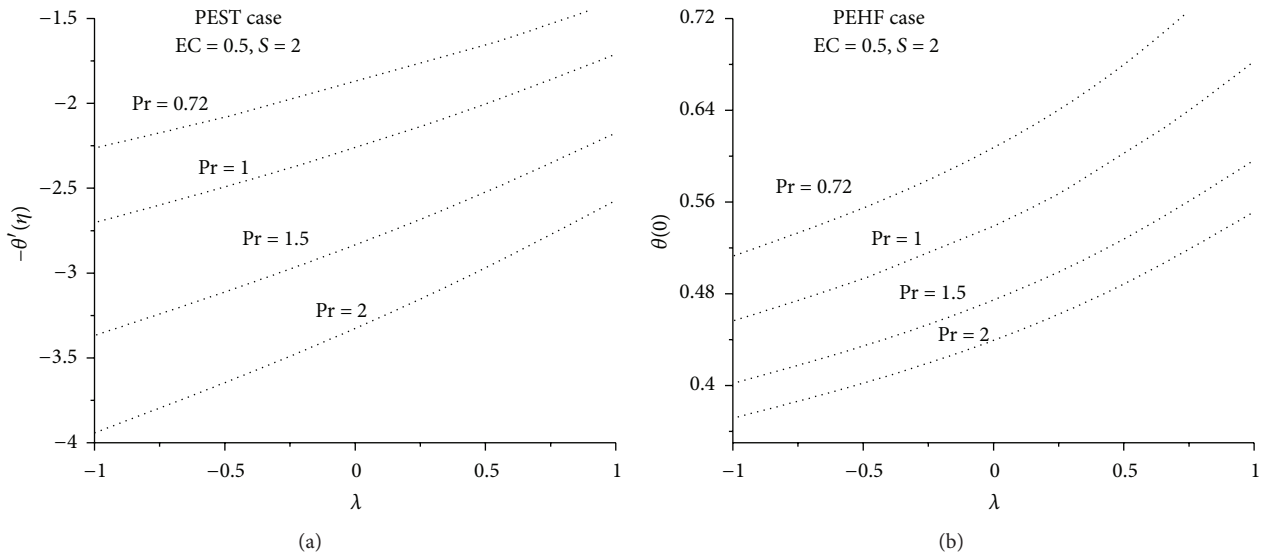

Figure 11: Heat transfer characteristics for different values of Pr and λ for both PEST and PEHF cases.

in the value of Pr. Hence Prandtl number can be used to increase the rate of cooling. Figure 9 explains the effect of viscous dissipation on temperature profiles. Viscous dissipation changes the temperature distribution by playing a role like an energy source, which leads to affect heat transfer rates. Here the temperature increases with increase in the value of Ec, due to the heat energy that is stored in the liquid and frictional heating, and this is true in both cases.

Figures 10(a) and 10(b) show the effect of internal heat source/sink parameter in the presence and in the absence of suction parameter S. This shows that there is an increase of temperature as λ increases, which results in the reduction of the thermal boundary layer thickness. It is also noticed that the temperature is less in presence of suction parameter than in absence of suction parameter.

The rate of heat transfer from the sheet that is evaluated by the variation of wall temperature gradient $\theta'(0)$ at sheet is present in Figure 11 for various values of Pr and λ. It is seen from this figure that the rate of heat transfer decreases with increases in Pr. It is also evident that $\theta'(0)$ which is negative means heat transfer and $\theta(0)$ which is positive means heat absorption, and also it is clear from Table 2. We have used the values of $\beta_T = 0.6$, $c_1 = 1$, $l = 0.1$, and $\rho = 1$ throughout our thermal analysis.

6. Conclusions

The present work deals with the boundary layer flow and heat transfer of a steady dusty fluid over an exponential stretching sheet with viscous dissipation and heat generation or absorption for both PEST and PEHF cases. The set of nonlinear ordinary differential equations (7), (15) for PEST case or (18) for PEHF case is solved numerically by applying RKF-45 order method using the software Maple. The results of the thermal characteristics at the wall are examined for the values of temperature gradient function $\theta'(0)$ in PEST case and the temperature function $\theta(0)$ in PEHF case, which are tabulated in Table 2. Also the results of skin friction coefficient $f''(0)$ are tabulated in Table 3 for various values of fluid particle interaction parameter (β) and suction parameter (S). The velocity and temperature profiles are obtained for various values of physical parameters like fluid-particle interaction parameter (β), Suction parameter (S), heat source/sink parameter (λ), Number density (N), Prandtl number (Pr), and Eckert number (Ec). The numerical results obtained are agrees with previously reported cases available in the literature [8, 14].

The major findings from the present study can be summarized as follows

(i) Suction parameter reduces the velocity and temperature profiles for both PEST and PEHF cases.

(ii) Heat source/sink effect is less in permeable than in impermeable stretching sheet.

(iii) The PEHF boundary condition is better suited for effective cooling of the stretching sheet.

(iv) The effect of increasing the values of β, Ec, and λ is to increase the wall temperature gradient function $\theta'(0)$ and wall temperature function $\theta(0)$ and decrease the increasing values of Pr and N both PEST and PEHF cases.

(v) The effect of heat source/sink on temperature is quite opposite to that of suction parameter.

(vi) If $\beta \to 0$, $N \to 0$, and $S \to 0$, then our results coincide with the results of Nadeem et al. [14] and Bidin and Nazar [8] for different values of Prandtl and Eckert numbers.

(vii) The effect of Ec increases, while Pr decreases the thermal boundary layer thickness.

(viii) Fluid phase temperature is higher than that of dust phase.

Acknowledgment

The authors would like to acknowledge the reviewers for their suggestions which lead to the present form of the manuscript. Further one of the co-author G. M. Pavithra gratefully acknowledges the financial support of Rajiv Gandhi National Fellowship (RGNF), UGC, New Delhi, India for pursuing this work.

References

[1] B. C. Sakiadis, "Boundary layer behaviour on continuous solid surface i. boundary-layer equations for two dimensional and axisymmetric flow," *AIChE Journal*, vol. 7, no. 1, pp. 26–28, 1961.

[2] B. C. Sakiadis, "Boundary layer behaviour on continuous solid surface ii, boundary layer behavior on continuous flat surface," *AIChE Journal*, vol. 7, no. 2, pp. 221–235, 1961.

[3] L. J. Crane, "Flow past a stretching plate," *Zeitschrift Für Angewandte Mathematik und Physik ZAMP*, vol. 21, no. 4, pp. 645–647, 1970.

[4] E. Magyari and B. Keller, "Heat and mass transfer in the boundary layers on an exponentially stretching continuous surface," *Journal of Physics D*, vol. 32, no. 5, pp. 577–585, 1999.

[5] E. M. A. Elbashbeshy, "Heat transfer over an exponentially stretching continuous surface with suction," *Archives of Mechanics*, vol. 53, no. 6, pp. 643–651, 2001.

[6] M. K. Partha, P. V. S. N. Murthy, and G. P. Rajasekhar, "Effect of viscous dissipation on the mixed convection heat transfer from an exponentially stretching surface," *Heat and Mass Transfer*, vol. 41, no. 4, pp. 360–366, 2005.

[7] E. Sanjayanand and S. K. Khan, "On heat and mass transfer in a viscoelastic boundary layer flow over an exponentially stretching sheet," *International Journal of Thermal Sciences*, vol. 45, no. 8, pp. 819–828, 2006.

[8] B. Bidin and R. Nazar, "Numerical solution of the boundary layer flow over an exponentially stretching sheet with thermal radiation," *European Journal of Scientific Research*, vol. 33, no. 4, pp. 710–717, 2009.

[9] M. A. Samad and M. Mohebujjaman, "MHD heat and mass transfer free convection flow along a vertical stretching sheet in presence of magnetic field with heat generation," *Research Journal of Applied Sciences*, vol. 1, no. 3, pp. 98–106, 2009.

[10] E. M. A. Elbashbeshy and D. A. Aldawody, "Heat transfer over an unsteady stretching surface with variable heat flux in the presence of a heat source or sink," *Computers and Mathematics with Applications*, vol. 60, no. 10, pp. 2806–2811, 2010.

[11] A. Ishak, "MHD boundary layer flow due to an exponentially stretching sheet with radiation effect," *Sains Malaysiana*, vol. 40, no. 4, pp. 391–395, 2011.

[12] A. R. P. Bala and R. N. Bhaskar, "Thermal radiation effects on hydro-magnetic flow due to an exponentially stretching sheet," *International Journal of Applied Mathematics*, vol. 3, no. 4, pp. 300–306, 2011.

[13] B. Sahoo and S. Poncet, "Flow and heat transfer of a third grade fluid past an exponentially stretching sheet with partial slip boundary condition," *International Journal of Heat and Mass Transfer*, vol. 54, no. 23-24, pp. 5010–5019, 2011.

[14] S. Nadeem, S. Zaheer, and T. Fang, "Effects of thermal radiation on the boundary layer flow of a Jeffrey fluid over an exponentially stretching surface," *Numerical Algorithms*, vol. 57, no. 2, pp. 187–205, 2011.

[15] H. Kumar, "Radiative heat transfer with hydromagnetic flow and viscous dissipation over a stretching surface in the presence of variable heat flux," *Thermal Science*, vol. 13, no. 2, pp. 163–169, 2009.

[16] K. Bhattacharyya, "Effects of radiation and heat source/sink on unsteady MHD boundary layer flow and heat transfer over a shrinking sheet with suction/injection," *Frontiers of Chemical Engineering in China*, vol. 5, no. 3, pp. 376–384, 2011.

[17] P. G. Saffman, "On the stability of laminar flow of a dusty gas," *Journal of Fluid Mechanics*, vol. 13, pp. 120–128, 1962.

[18] N. Datta and S. K. Mishra, "Boundary layer flow of a dusty fluid over a semi-infinite flat plate," *Acta Mechanica*, vol. 42, no. 1-2, pp. 71–83, 1982.

[19] B. J. Gireesha, G. K. Ramesh, S. Abel, and C. S. Bagewadi, "Boundary layer flow and heat transfer of a dusty fluid flow over a stretching sheet with non-uniform heat source/sink," *International Journal of Multiphase Flow*, vol. 37, no. 8, pp. 977–982, 2011.

[20] B. J. Gireesha, G. K. Ramesh, and C. S. Bagewadi, "Heat transfer in MHD flow of a dusty fluid over a stretching sheet with viscous dissipation," *Journal of Applied Sciences Research*, vol. 3, no. 4, pp. 2392–2401, 2012.

[21] B. J. Gireesha, G. S. Roopa, and C. S. Bagewadi, "Effect of viscous dissipation and heat source on flow and heat transfer of dusty fluid over unsteady stretching sheet," *Applied Mathematics and Mechanics*, vol. 33, no. 8, pp. 1001–1014, 2012.